Title

A Lytic Viral Long Noncoding RNA Modulates the Function of a Latent Protein

Journal

Journal of Virology, 88(3)

ISSN

0022-538X

Authors

Campbell, Mel
Kim, Kevin Y
Chang, Pei-Ching
et al.

Publication Date

2014-02-01

DOI

10.1128/jvi.03251-13

Peer reviewed

JVI Journals.ASM.org

A Lytic Viral Long Noncoding RNA Modulates the Function of a Latent Protein

Mel Campbell,[a,b] Kevin Y. Kim,[a,b] Pei-Ching Chang,[d] Steve Huerta,[a,b] Bogdan Shevchenko,[a,b] Don-Hong Wang,[a,b] Chie Izumiya,[a,b] Hsing-Jien Kung,[b,c,e,f] Yoshihiro Izumiya[a,b,c]

Department of Dermatology,[a] UC Davis Cancer Center,[b] and Department of Biochemistry and Molecular Medicine,[c] University of California, Davis, California, USA; Institute of Microbiology and Immunology, National Yang-Ming University, Taipei, Taiwan[d]; National Health Research Institutes, Maioli, Taiwan[e]; Taipei Medical University, Taipei, Taiwan[f]

Latent Kaposi's sarcoma-associated herpesvirus (KSHV) episomes are coated with viral latency-associated nuclear antigen (LANA). In contrast, LANA rapidly disassociates from episomes during reactivation. Lytic KSHV expresses polyadenylated nuclear RNA (PAN RNA), a long noncoding RNA (lncRNA). We report that PAN RNA promotes LANA-episome disassociation through an interaction with LANA which facilitates LANA sequestration away from KSHV episomes during reactivation. These findings suggest that KSHV may have evolved an RNA aptamer to regulate latent protein function.

Kaposi's sarcoma-associated herpesvirus (KSHV; also called human herpesvirus 8) is a gammaherpesvirus linked to Kaposi's sarcoma (KS) and two lymphoproliferative disorders, primary effusion lymphoma (PEL; also called body cavity B lymphoma [BCBL]) and a subset of multicentric Castleman's disease (1). Pervasive transcription, which generates a wide variety of transcripts with little apparent protein-coding potential, has been observed on a genome-wide scale in beta- and gammaherpesviruses, including human cytomegalovirus (HCMV) (2) and KSHV (3, 4), during lytic growth. One class of noncoding RNAs, called long noncoding RNAs (lncRNAs), are defined as RNA polymerase II (Pol II)-transcribed noncoding RNAs greater than 200 nucleotides in length (5). KSHV encodes a viral lncRNA known as polyadenylated nuclear RNA (PAN RNA), an abundant early gene product. Although PAN RNA was first described 17 years ago (6), its discovery predated the widespread recognition of noncoding RNAs. However, recent studies have begun to focus on the role of PAN RNA in the KSHV life cycle. PAN RNA has been reported to play a role in KSHV gene expression, replication, and immune modulation (7–9). PAN RNA binds the transcription factor IRF4 (8), lysine demethylases UTX and JMJD3, and the lysine methyltransferase MLL2 (9), in support of the notion that, similar to cellular lncRNAs, PAN RNA interacts with transcriptional regulators and chromatin modifiers to modulate viral gene expression. Moreover, recent mapping studies have found widespread PAN RNA interaction sites on the KSHV episome as well as the host genome, and PAN RNA expression is required for optimal expression of the entire KSHV lytic gene expression program (10).

Previously, we performed a large-scale coimmunoprecipitation (co-IP) analysis to identify latency-associated nuclear antigen (LANA)-interacting protein partners using stably LANA-expressing HeLa cells (11). In the experiment, RNA-binding factors such as hnRNPs, SF3B1, THRAP3, and DHX15 were found to be among LANA-interacting proteins. The result raised the questions of whether LANA possesses the property of RNA binding and whether LANA interacts with PAN RNA. To address this, the ability of LANA to interact with PAN RNA was evaluated *in vitro* and *in vivo*. In order to perform *in vitro* interaction analyses, full-length LANA was expressed using recombinant baculovirus and purified by FLAG-M2 resin (Flag-LANA) (Fig. 1A). Purified Flag-LANA was incubated with PAN RNA that had been biotinylated *in vitro*. The interaction was captured using avidin-coated magnetic beads followed by immunoblot detection of precipitated LANA with anti-Flag antibody (Fig. 1B, panel a). As shown in Fig. 1B (panel b), an interaction between LANA and PAN RNA was detected *in vitro*. LANA exhibited a preference for sense (S) PAN RNA over antisense (AS) PAN RNA, and there was no interaction of LANA with streptavidin beads. We then searched for an endogenous interaction between PAN RNA and LANA in naturally infected BCBL-1 cells using RNA cross-linking immunoprecipitation (RNA CLIP) (Fig. 1C, panel a). Before and after reactivation, BCBL-1 cells were fixed with 0.3% formaldehyde, and RNA/LANA complexes were precipitated with anti-LANA antibody. Several other antibodies, including preimmune (PI) rabbit IgG, were also used in these experiments. The amount of precipitated PAN RNA was measured by reverse transcription-quantitative PCR (RT-qPCR) after reverse cross-linking and purification of RNA from the protein-RNA complexes. The results clearly showed that PAN RNA interacts with LANA during reactivation (Fig. 1C, panel b). There was also an interaction between PAN RNA and K-Rta; however, no PAN RNA interaction was detected using PI, SUMO-1, SUMO-2/3, or K-bZIP antibodies. The RNA CLIP uses RT-qPCR to detect coprecipitating RNAs, so due to the high sensitivity of the assay, we can detect other RNAs in LANA RNA immunoprecipitations (RIPs). However, we compared the RIP/input ratio for several RNAs in LANA RIPs and found that the RIP/input ratio for PAN RNA is three times greater than for GAPDH mRNA, five times greater than for K-bZIP mRNA, and three times greater than for LANA mRNA. The PAN RNA binding domain of LANA was then determined. A series of glutathione *S*-transferase (GST)-LANA deletion proteins were incubated with biotinylated PAN RNA and interacting GST fusion proteins were

Received 14 November 2013 **Accepted** 18 November 2013
Published ahead of print 20 November 2013
Address correspondence to Yoshihiro Izumiya, yizumiya@ucdavis.edu.

doi:10.1128/JVI.03251-13

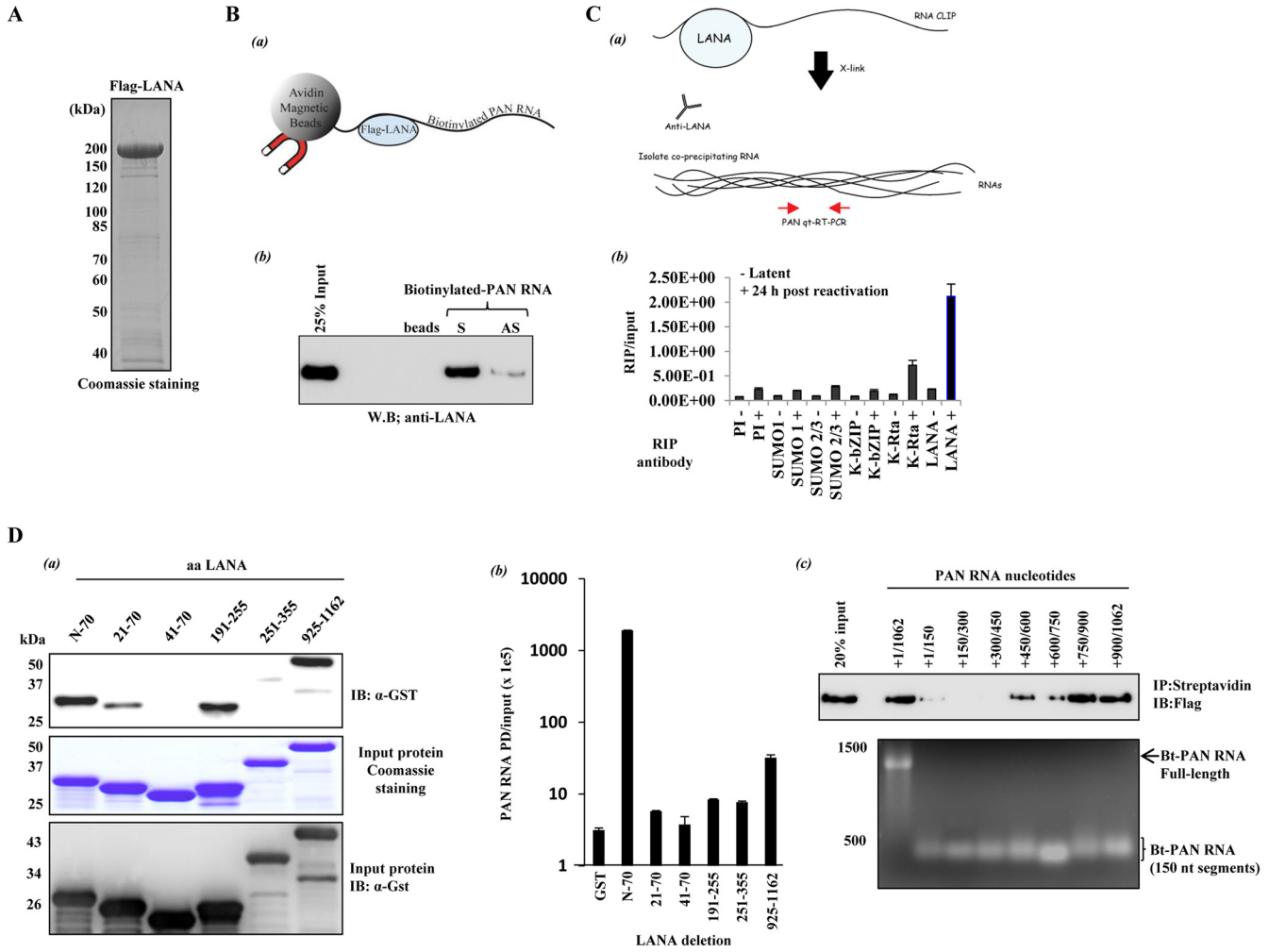

FIG 1 LANA-PAN RNA interaction. (A) Flag-LANA expression. Flag-LANA was produced from baculovirus-infected Sf9 cells. LANA was purified on FLAG-M2 resin and analyzed by SDS-PAGE with Coomassie brilliant blue staining. (B) *In vitro* LANA-PAN RNA interaction. (a) Illustration of the reaction. (b) Purified Flag-LANA was incubated with biotinylated S or AS PAN RNA. The interaction was captured with streptavidin magnetic beads and probed with anti-Flag. "beads" indicates the incubation of streptavidin beads plus Flag-LANA. (C) *In vivo* LANA-PAN interaction analyzed by RNA CLIP. (a) Illustration of the reaction. (b) Before (−) and after (+) 24 h chemical reactivation, BCBL-1 cells were fixed with 0.3% formaldehyde, and RNA-LANA complexes were precipitated with the indicated antibodies. After the reversal of cross-links and purification of RNA from the protein-RNA complexes, the amount of precipitated PAN RNA was measured by RT-qPCR using PAN RNA-specific primers. Values are the means and standard deviations (SD) from 3 determinations. (D) Mapping the LANA- and PAN RNA-interacting domains. (a) LANA-interacting domain. GST pulldown (PD)-protein capture. GST-LANA deletion fusion proteins were produced in *Escherichia coli*, purified on glutathione Sepharose, and eluted from the beads with glutathione. The fusion proteins were incubated with *in vitro*-transcribed biotinylated PAN RNA, and complexes were isolated with magnetic streptavidin beads. Captured protein was detected with anti-GST antibody (top). Purified proteins used in these reactions are shown by staining with Coomassie (middle) and immunoblotting with anti-GST (bottom). (b) GST-PD-RNA capture. After PD and washing, the GST fusion beads were processed for quantification of bound RNA. Captured PAN RNA was quantified by RT-qPCR. LANA amino acid residues in each deletion are listed in panels a and b. (c) Mapping of PAN RNA nucleotides that interact with LANA. PD was carried out with full-length Flag-LANA plus *in vitro*-transcribed, biotinylated PAN RNA fragments. The endpoints of each PAN RNA are given. Anti-Flag analysis of the pull-down (top) and denaturing agarose gel-ethidium bromide staining of the *in vitro* transcribed RNAs utilized (bottom) are shown.

probed with anti-GST antibody. PAN RNA predominantly captured the extreme N and C termini of LANA in pulldown assays (Fig. 1D, panel a), regions previously identified as LANA chromosome-binding domains (12, 13). The reciprocal analysis was also performed, in which the amount of PAN RNA that was captured by a given GST-LANA deletion was quantified. Following the *in vitro* incubation with LANA deletions, precipitated PAN RNA was measured by RT-qPCR. The N-terminal region of LANA (residues 1 to 70) but not the portion of LANA encoding residues 20 to 71 precipitated PAN RNA more than 600-fold compared with the GST control (Fig. 1D, panel b). These results suggest that the N-terminal 20 amino acids of LANA are crucial for PAN RNA interaction and that N-terminal residues 1 to 70 contain an RNA-binding domain of LANA. Although less robust, the C terminus of LANA also captured 10-fold more PAN RNA than the GST control (Fig. 1D, panel b). These results suggest that there are independent N- and C-terminal LANA RNA-binding domains. By using a series of biotinylated PAN RNA deletions and full-length LANA, the interacting region of PAN RNA was then mapped to RNA segments toward the 3′ end of PAN contained within nucleotides 750 to 1062 (Fig. 1D, panel c). Using ChIP (chromatin immunoprecipitation)-on-KSHV chip approaches, our lab previ-

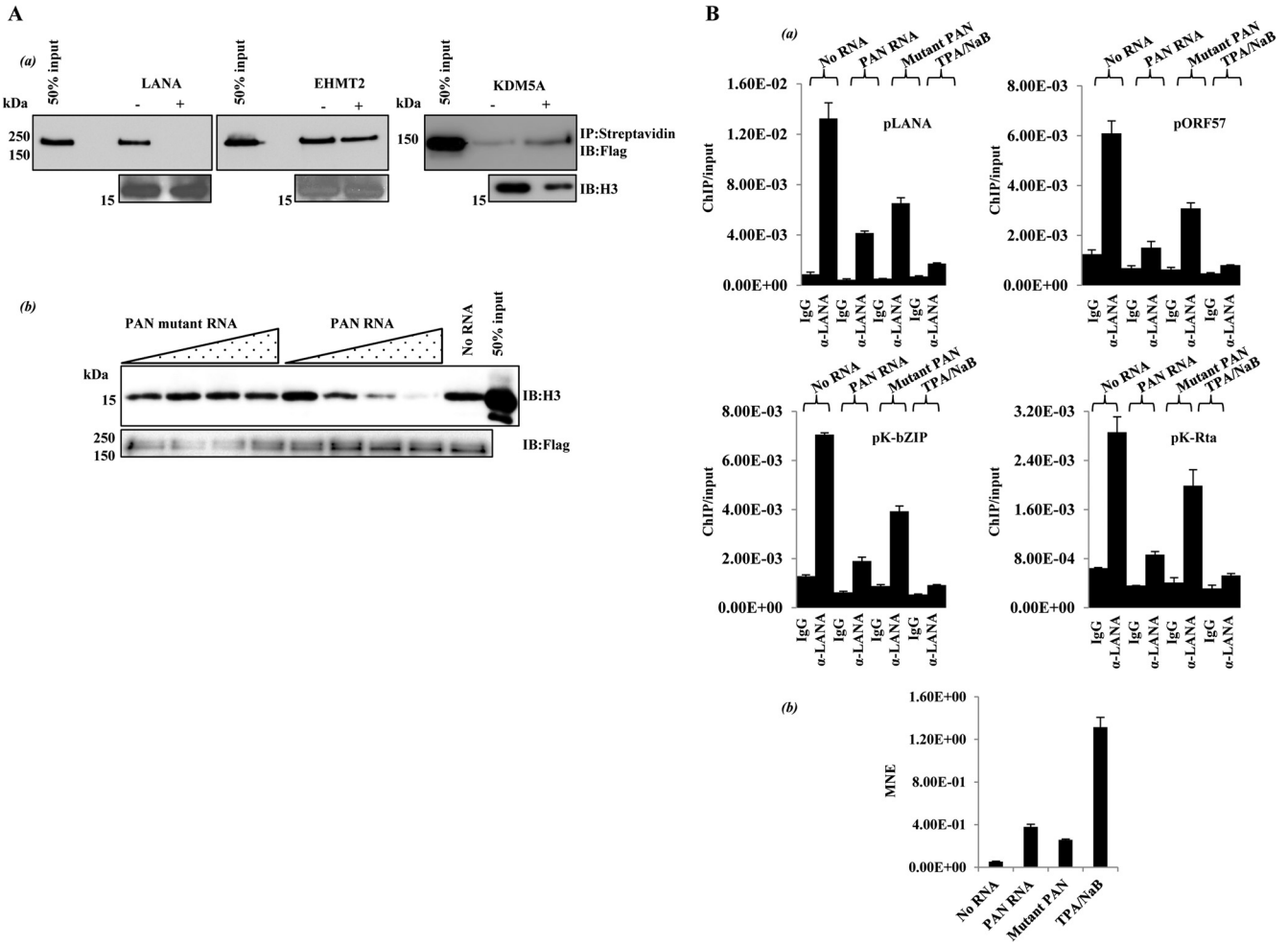

FIG 2 PAN RNA influences LANA-histone interaction *in vitro* and *in vivo*. (A) *In vitro*. (a) Histone binding reactions (14) were carried out using the purified proteins indicated. Biotinylated histone H3 (Active Motif) was used as the binding substrate. − and +, presence and absence of unlabeled PAN RNA competitor. Complexes were captured with streptavidin beads and analyzed by immunoblotting. (b) Mutant PAN lacks activity. Histone binding reaction mixtures with Flag LANA beads and histone H3 contained 0, 0.5, 5, 50, or 500 nM *in vitro*-transcribed, unlabeled PAN RNA or a non-LANA-interacting PAN RNA fragment (PAN nucleotides 300 to 450). After washing, bound H3 was analyzed by immunoblotting. (B) *In vivo*. (a) Latent 293T/rKSHV.219 cells were nucleofected (Lonza Nucleofector) with *in vitro*-transcribed PAN RNA or mutant PAN RNA (PAN nucleotides 300 to 450) (0.5 μM RNA), and an ORF57 expression vector DNA. Eighteen hours later, the cells were fixed as described in the Fig. 1 legend and processed for LANA ChIP, and eluted DNA was analyzed by qPCR. The amount of immunoprecipitated, amplified DNA relative to input is listed for 4 KSHV genomic loci (means and SD from 3 determinations). Chemical reactivation (3 mM sodium butyrate [NaB] and 20 ng/ml 12-*O*-tetradecanoylphorbol acetate [TPA]) was used as a positive control. (b) Nucleofected PAN RNA expression. Prior to fixation for ChIP, a small amount of each cell culture was harvested for RNA isolation. cDNA was prepared and analyzed for PAN or mutant PAN RNA expression by qPCR (MNE, mean normalized expression; reference, β-actin).

ously demonstrated that KSHV LANA occupies a large portion of the KSHV episome during latency and this association is rapidly lost during the initial stages of K-Rta-mediated reactivation (14). The overlapping kinetics of PAN RNA expression (15) and LANA-episome disassociation (14), in addition to the extremely abundant nature of PAN RNA expression (6, 15), prompted us to ask whether PAN RNA is involved in LANA-episome sequestration. First, using an *in vitro* approach, we found that PAN RNA inhibits the interaction of purified LANA with histone H3 (Fig. 2A, panel a). As controls, we examined the effect of PAN RNA on H3 binding by the histone-modifying proteins EHMT2 (16) and KDM5A (17), which are known to interact directly with H3. We confirmed that the effect of PAN on protein-H3 interaction is not universal, as PAN RNA had little or no effect on H3 binding by EHMT2 or KDM5A (Fig. 2A, panel a). In addition, when assayed over a range of PAN RNA concentrations that inhibited the LANA-H3 interaction, a mutant PAN RNA fragment that did not interact with LANA *in vitro* (PAN nucleotides 300 to 450) (Fig. 1D, panel c) was without effect on LANA-H3 binding (Fig. 2A, panel b). Enforced expression of PAN RNA in latent 293T/rKSHV.219 cells (Fig. 2B, panel b) also resulted in a reduction in LANA occupancy at several KSHV promoters *in vivo* (Fig. 2B, panel a). Moreover, mutant PAN RNA was not as effective as full-length PAN RNA in removal of LANA from latent KSHV episomes (Fig. 2B, panel a). The dynamic nature of the LANA-episome interaction that was previously determined by hybridization (14) was also confirmed by ChIP analyses with anti-LANA antibody. By using K-Rta-inducible BCBL-1 cells (18), the amount of precipitated viral DNA was measured by qPCR amplification before reactivation and at 8 h postreactivation, and several

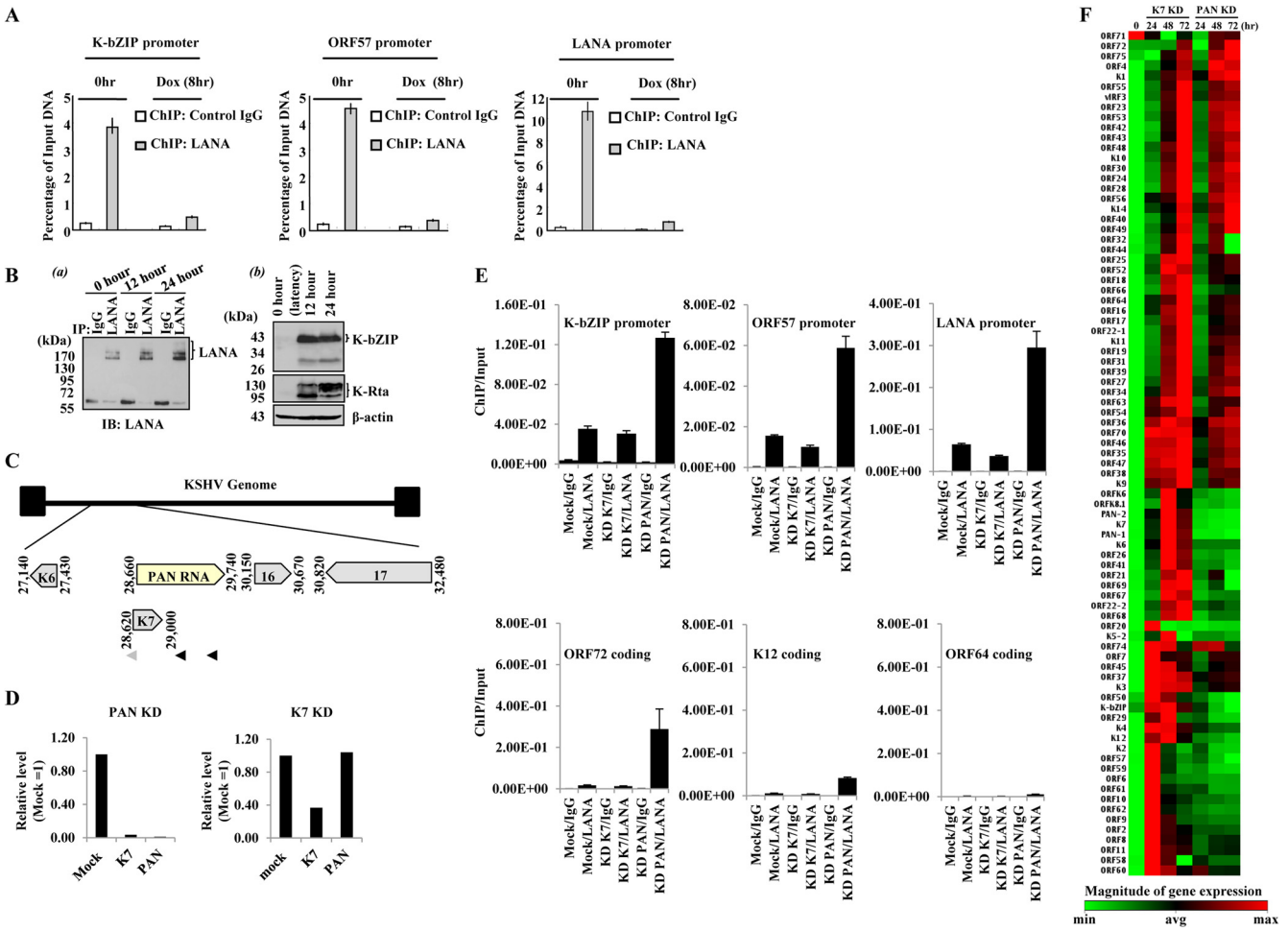

FIG 3 LANA-episome dynamics. (A) KSHV episome-LANA dynamics during reactivation. Anti-LANA and control IgG ChIP DNAs were prepared from K-Rta-inducible BCBL-1 cells at 0 and 8 h after K-Rta-mediated reactivation. The immunoprecipitated DNA was analyzed by qPCR using primer pairs against the KSHV ORFs listed. Values are the percentage of input DNA. Values are derived from the ratio of the threshold cycle (C_T) values of the amplified DNA immunoprecipitated with each antibody relative to the amount of input DNA amplified. (B) (a) LANA protein levels during the early stages of reactivation. K-Rta-inducible BCBL-1 cell lysates were prepared at the indicated times, immunoprecipitated with the indicated antibodies, and probed with anti-LANA antibody. (b) Verification of reactivation. K-Rta-inducible BCBL-1 cell lysates were prepared at the indicated times. Immunoblots were probed with the indicated antibodies. (C) KSHV PAN RNA genomic organization. An expanded view of the K7/PAN locus is shown, and the positions of K7 KD (gray arrowhead) and PAN RNA KD oligonucleotides (black arrowheads) are shown. (D to F) PAN RNA KD alters LANA occupancy of KSHV episomes and viral gene expression. (D) PAN RNA and K7 knockdown. iSLK/rKSHV.219 cells were nucleofected with PAN or K7 antisense oligonucleotides and reactivated by doxycycline addition. At 48 h postreactivation, PAN and K7 gene expression was analyzed by qPCR. PAN RNA KD affects both K7 and PAN RNA transcript levels; K7 knockdown affects only K7 mRNAs. The expression level relative to that obtained with mock nucleofection is shown. (E) LANA ChIP. BCBL-1 cells were nucleofected with antisense PAN RNA or K7 control oligonucleotides 24 h prior to chemical reactivation. Cells were fixed with 0.3% formaldehyde after 24 h chemical reactivation, and chromatin was immunoprecipitated with control IgG or rat anti-LANA IgG. The immunoprecipitated DNA was isolated and quantitated by qPCR. The amount of immunoprecipitated DNA relative to input is listed for each KSHV locus examined. Values are the means and SD from 3 determinations. (F) KSHV gene expression array. After PAN/K7 KD and reactivation, RNA was harvested at 24, 48, and 72 h and reverse transcribed, and cDNAs were analyzed with a KSHV gene expression array. A clustergram was generated from the data set using nonsupervised hierarchical clustering. A heat map depicting relative expression levels with dendrograms is shown. RNA prepared from mock nucleofected, nonreactivated BCBL-1 cells served as the latent (0-h) control (normalized expression; green, low; red, high).

KSHV genomic loci were selected for analysis (Fig. 3A). As a control, we examined the total amount of LANA by immunoblotting. The results showed that the overall level of LANA protein did not decrease during the period of LANA-episome disassociation (Fig. 3B, panel a). In addition, detection of lytic gene expression provided confirmation of ongoing reactivation (Fig. 3B, panel b). Taken together, these results (Fig. 1 to 3) suggest that (i) PAN RNA interacts with LANA, (ii) LANA disassociates from the KSHV genome during lytic replication, and (iii) the PAN-LANA interaction is important for this partitioning. We then employed a previously described knockdown (KD) procedure using 2′-O-methyl- and phosphothioate-substituted modified antisense oligonucleotides and endogenous RNase H activity to target PAN RNA. As previously noted (7), KD of PAN RNA is complicated due to the overlapping nature of the K7/survivin transcript (19) (Fig. 3C), and we confirmed that PAN RNA KD also results in K7 KD (Fig. 3D). To distinguish between the effects of PAN RNA and the K7/survivin protein, an additional oligonucleotide that specifically targets the K7 transcript, upstream of the overlapping region, was utilized as a control. The K7 antisense oligonucleotide

decreases K7 mRNA but not PAN RNA expression (Fig. 3D). BCBL-1 cells were nucleofected with antisense PAN RNA or K7 control oligonucleotides 24 h prior to chemical reactivation with sodium butyrate and phorbol myristate acetate. After the 24-h reactivation, each culture was fixed with 0.3% formaldehyde and processed for ChIP. The LANA ChIP (Fig. 3E) showed that PAN RNA KD resulted in greater recovery of KSHV DNA at several distinct KSHV loci relative to the K7 control KD or mock nucleofection controls. This result is consistent with the notion that optimal levels of PAN RNA are needed for LANA sequestration away from KSHV episomes during the early stages of reactivation. The low level of ORF64 DNA amplified in the LANA ChIP is consistent with a low level of LANA occupancy observed in this region during latency (14). Next, the effect of PAN RNA KD on viral gene expression was examined at 24 to 72 h postreactivation following the KD/reactivation regime described above. We utilized KSHV PCR arrays (20, 21) to cover all KSHV open reading frames. As shown in Fig. 3F, PAN RNA KD resulted in an overall decrease of viral gene expression at each time point compared to K7 KD controls. We have also conducted this KD experiment using iSLK/rKSHV.219 cells (22) using inducible K-Rta expression as a means of reactivation and have obtained results similar to those obtained with chemical reactivation (data not shown). This suggests that LANA-episome disassociation is not simply the result of changes in histone acetylation patterns.

In the present study, we showed that lytic lncRNA is at least in part responsible for the LANA-episome dissociation during reactivation, which may have profound effects on viral gene expression (7, 9). PAN RNA knockdown during reactivation was accompanied by higher levels of episome-associated LANA and reduced viral gene expression; this is consistent with a repressive role of LANA in lytic gene expression in general (23). Of note, we also noticed that a few viral gene expression patterns did not follow the same trend in our PCR array analyses, which is consistent with a previous report (10), indicating that PAN RNA may have other functions. Importantly, similar to viral gene regulation, Affymetrix human gene expression arrays showed that PAN RNA also regulates cellular gene expression targeted by LANA (data not shown). Using rKSHV.219 indicator cells, we noted that the introduction of a bolus of PAN RNA (with or without ORF57 expression) or PAN RNA expression vectors in an otherwise latent KSHV-positive cell is insufficient to induce viral reactivation (data not shown). These results indicate that PAN RNA expression, *per se*, cannot bypass the need for K-Rta to initiate reactivation. Interestingly, using a PAN RNA deletion KSHV bacmid, Rossetto and colleagues have shown that this recombinant virus cannot express the entire KSHV lytic program, nor can complementation by K-Rta overexpression be achieved (9, 10). Although PAN RNA is considered to be a K-Rta-responsive downstream target, these results suggest that a certain low level of PAN RNA is required for K-Rta expression to initiate the lytic program. It will be important to examine whether PAN RNA directly regulates K-Rta transcription function, as we observed that PAN RNA also interacts with K-Rta during reactivation (Fig. 1C, panel b). Although the exact structural elements of PAN RNA that are recognized by LANA are unclear, we hypothesize that the extreme abundance of PAN RNA (6, 15) as well as other PAN RNA-interacting proteins or specific secondary structures of PAN RNA dictate the specificity of the PAN RNA-LANA interaction. This idea is also supported by the recent development of RNA aptamers, which are synthesized to specifically recognize a particular target protein. It is possible that the virus has naturally adapted the strategy and evolved a specific RNA to dampen the latent protein function during its lytic phase. A similar phenotype has also been reported with a cellular noncoding RNA, GAS5, which specifically associates with the DNA-binding domain of the glucocorticoid receptor (GR) to counteract the GR transcription function (24). We propose that one of the functions of PAN RNA is to modulate the activity of LANA as cells switch from latency to lytic replication.

ACKNOWLEDGMENTS

This work was supported by grants from the National Institutes of Health (CA14779 to Y.I. and DE19085 to H.J.K. and Y.I.) and by an American Cancer Society Research Scholar Grant (RSG-13-383-01-MPC) to Y.I. This work was also partially supported by a grant from the Department of Defense (W81XWH1110575 to Y.I.). Additional funding was provided by a Cancer Center Support Grant (P30 CA93373).

REFERENCES

1. **Ganem D.** 2010. KSHV and the pathogenesis of Kaposi sarcoma: listening to human biology and medicine. J. Clin. Invest. **120:**939–949. http://dx.doi.org/10.1172/JCI40567.
2. **Zhang G, Raghavan B, Kotur M, Cheatham J, Sedmak D, Cook C, Waldman J, Trgovcich J.** 2007. Antisense transcription in the human cytomegalovirus transcriptome. J. Virol. **81:**11267–11281. http://dx.doi.org/10.1128/JVI.00007-07.
3. **Chandriani S, Xu Y, Ganem D.** 2010. The lytic transcriptome of Kaposi's sarcoma-associated herpesvirus reveals extensive transcription of noncoding regions, including regions antisense to important genes. J. Virol. **84:**7934–7942. http://dx.doi.org/10.1128/JVI.00645-10.
4. **Lin YT, Kincaid RP, Arasappan D, Dowd SE, Hunicke-Smith SP, Sullivan CS.** 2010. Small RNA profiling reveals antisense transcription throughout the KSHV genome and novel small RNAs. RNA **16:**1540–1558. http://dx.doi.org/10.1261/rna.1967910.
5. **Kapranov P, Cheng J, Dike S, Nix DA, Duttagupta R, Willingham AT, Stadler PF, Hertel J, Hackermuller J, Hofacker IL, Bell I, Cheung E, Drenkow J, Dumais E, Patel S, Helt G, Ganesh M, Ghosh S, Piccolboni A, Sementchenko V, Tammana H, Gingeras TR.** 2007. RNA maps reveal new RNA classes and a possible function for pervasive transcription. Science **316:**1484–1488. http://dx.doi.org/10.1126/science.1138341.
6. **Sun R, Lin SF, Gradoville L, Miller G.** 1996. Polyadenylylated nuclear RNA encoded by Kaposi sarcoma-associated herpesvirus. Proc. Natl. Acad. Sci. U. S. A. **93:**11883–11888. http://dx.doi.org/10.1073/pnas.93.21.11883.
7. **Borah S, Darricarrere N, Darnell A, Myoung J, Steitz JA.** 2011. A viral nuclear noncoding RNA binds re-localized poly(A) binding protein and is required for late KSHV gene expression. PLoS Pathog. **7:**e1002300. http://dx.doi.org/10.1371/journal.ppat.1002300.
8. **Rossetto CC, Pari GS.** 2011. Kaposi's sarcoma-associated herpesvirus noncoding polyadenylated nuclear RNA interacts with virus- and host cell-encoded proteins and suppresses expression of genes involved in immune modulation. J. Virol. **85:**13290–13297. http://dx.doi.org/10.1128/JVI.05886-11.
9. **Rossetto CC, Pari G.** 2012. KSHV PAN RNA associates with demethylases UTX and JMJD3 to activate lytic replication through a physical interaction with the virus genome. PLoS Pathog. **8:**e1002680. http://dx.doi.org/10.1371/journal.ppat.1002680.
10. **Rossetto CC, Tarrant-Elorza M, Verma S, Purushothaman P, Pari GS.** 2013. Regulation of viral and cellular gene expression by Kaposi's sarcoma-associated herpesvirus polyadenylated nuclear RNA. J. Virol. **87:**5540–5553. http://dx.doi.org/10.1128/JVI.03111-12.
11. **Kim KY, Huerta SB, Izumiya C, Wang DH, Martinez A, Shevchenko B, Kung HJ, Campbell M, Izumiya Y.** 2013. Kaposi's sarcoma-associated herpesvirus (KSHV) latency-associated nuclear antigen regulates KSHV epigenome by association with the histone demethylase KDM3A. J. Virol. **87:**6782–6793. http://dx.doi.org/10.1128/JVI.00011-13.
12. **Barbera AJ, Ballestas ME, Kaye KM.** 2004. The Kaposi's sarcoma-associated herpesvirus latency-associated nuclear antigen 1 N terminus is essential for chromosome association, DNA replication, and episome persistence. J. Virol. **78:**294–301. http://dx.doi.org/10.1128/JVI.78.1.294-301.2004.

13. **Kelley-Clarke B, De Leon-Vazquez E, Slain K, Barbera AJ, Kaye KM.** 2009. Role of Kaposi's sarcoma-associated herpesvirus C-terminal LANA chromosome binding in episome persistence. J. Virol. **83:**4326–4337. http://dx.doi.org/10.1128/JVI.02395-08.
14. **Campbell M, Chang PC, Huerta S, Izumiya C, Davis R, Tepper CG, Kim KY, Shevchenko B, Wang DH, Jung JU, Luciw PA, Kung HJ, Izumiya Y.** 2012. Protein arginine methyltransferase 1-directed methylation of Kaposi sarcoma-associated herpesvirus latency-associated nuclear antigen. J. Biol. Chem. **287:**5806–5818. http://dx.doi.org/10.1074/jbc.M111.289496.
15. **Song MJ, Brown HJ, Wu TT, Sun R.** 2001. Transcription activation of polyadenylated nuclear RNA by Rta in human herpesvirus 8/Kaposi's sarcoma-associated herpesvirus. J. Virol. **75:**3129–3140. http://dx.doi.org/10.1128/JVI.75.7.3129-3140.2001.
16. **Collins RE, Northrop JP, Horton JR, Lee DY, Zhang X, Stallcup MR, Cheng X.** 2008. The ankyrin repeats of G9a and GLP histone methyltransferases are mono- and dimethyllysine binding modules. Nat. Struct. Mol. Biol. **15:**245–250. http://dx.doi.org/10.1038/nsmb.1384.
17. **Christensen J, Agger K, Cloos PA, Pasini D, Rose S, Sennels L, Rappsilber J, Hansen KH, Salcini AE, Helin K.** 2007. RBP2 belongs to a family of demethylases, specific for tri- and dimethylated lysine 4 on histone 3. Cell **128:**1063–1076. http://dx.doi.org/10.1016/j.cell.2007.02.003.
18. **Nakamura H, Lu M, Gwack Y, Souvlis J, Zeichner SL, Jung JU.** 2003. Global changes in Kaposi's sarcoma-associated virus gene expression patterns following expression of a tetracycline-inducible Rta transactivator. J. Virol. **77:**4205–4220. http://dx.doi.org/10.1128/JVI.77.7.4205-4220.2003.
19. **Wang HW, Sharp TV, Koumi A, Koentges G, Boshoff C.** 2002. Characterization of an anti-apoptotic glycoprotein encoded by Kaposi's sarcoma-associated herpesvirus which resembles a spliced variant of human survivin. EMBO J. **21:**2602–2615. http://dx.doi.org/10.1093/emboj/21.11.2602.
20. **Fakhari FD, Dittmer DP.** 2002. Charting latency transcripts in Kaposi's sarcoma-associated herpesvirus by whole-genome real-time quantitative PCR. J. Virol. **76:**6213–6223. http://dx.doi.org/10.1128/JVI.76.12.6213-6223.2002.
21. **Dittmer DP.** 2003. Transcription profile of Kaposi's sarcoma-associated herpesvirus in primary Kaposi's sarcoma lesions as determined by real-time PCR arrays. Cancer Res. **63:**2010–2015. http://cancerres.aacrjournals.org/content/63/9/2010.long.
22. **Myoung J, Ganem D.** 2011. Generation of a doxycycline-inducible KSHV producer cell line of endothelial origin: maintenance of tight latency with efficient reactivation upon induction. J. Virol. Methods **174:**12–21. http://dx.doi.org/10.1016/j.jviromet.2011.03.012.
23. **Li Q, Zhou F, Ye F, Gao SJ.** 2008. Genetic disruption of KSHV major latent nuclear antigen LANA enhances viral lytic transcriptional program. Virology **379:**234–244. http://dx.doi.org/10.1016/j.virol.2008.06.043.
24. **Kino T, Hurt DE, Ichijo T, Nader N, Chrousos GP.** 2010. Noncoding RNA gas5 is a growth arrest- and starvation-associated repressor of the glucocorticoid receptor. Sci. Signal. **3:**ra8. http://dx.doi.org/10.1126/scisignal.2000568.